



저작자표시-비영리-변경금지 2.0 대한민국

이용자는 아래의 조건을 따르는 경우에 한하여 자유롭게

- 이 저작물을 복제, 배포, 전송, 전시, 공연 및 방송할 수 있습니다.

다음과 같은 조건을 따라야 합니다:



저작자표시. 귀하는 원저작자를 표시하여야 합니다.



비영리. 귀하는 이 저작물을 영리 목적으로 이용할 수 없습니다.



변경금지. 귀하는 이 저작물을 개작, 변형 또는 가공할 수 없습니다.

- 귀하는, 이 저작물의 재이용이나 배포의 경우, 이 저작물에 적용된 이용허락조건을 명확하게 나타내어야 합니다.
- 저작권자로부터 별도의 허가를 받으면 이러한 조건들은 적용되지 않습니다.

저작권법에 따른 이용자의 권리는 위의 내용에 의하여 영향을 받지 않습니다.

이것은 [이용허락규약\(Legal Code\)](#)을 이해하기 쉽게 요약한 것입니다.

[Disclaimer](#)

Thesis for the Degree of Master of Physics

Crystallization Management with
Tailored Thermal Annealing for
Quasi-Two-Dimensional
Perovskites Light-Emitting Diodes

by

Yeong Gyeong Kim

Department of Physics

The Graduate School

Pukyong National University

February, 2024

Crystallization Management with Tailored Thermal Annealing for Quasi-Two-Dimensional Perovskites Light-Emitting Diodes

(준 2차원 페로브스카이트
발광다이오드를 위한 맞춤형
열처리를 통한 결정화 제어)

Advisor: Prof. Sung Heum Park

By

Yeong Gyeong Kim

A thesis submitted in partial fulfillment of the requirements

for the degree of

Master of Physics

in Department of Physics, The Graduate School,

Pukyong National University

February 2024

김영경의 이학석사 학위논문을
인준함.

2024년 2월 16일

위원장 이보람

위원 박성흠

위원 김정환

Crystallization Management with Tailored Thermal
Annealing for Quasi-Two-Dimensional Perovskites
Light-Emitting Diodes

A dissertation

by

Yeong Gyeong Kim

Approved by

(Chairman) **Bo Ram Lee**

(Member) **Sung Heum Park**

(Member) **Jung Hwan Kim**

February 16th, 2024

Contents

Contents	i
List of Figures	iii
List of Tables	iv
Abstract	v
1. Introduction	1
1.1. Perovskites.....	1
1.2. Light-Emitting Diodes.....	9
2. Experimental Section	14
2.1 Materials.....	14
2.2 Device Fabrication.....	14
3. Result and Discussion	16
3.1 Device Structure of Quasi-2D Perovskite Light-Emitting Diodes.....	16
3.2 Characteristics of Quasi-2D Perovskite Films with Thermal Annealing .	16
3.3 Characteristics of Quasi-2D Perovskite Light-Emitting Diodes with Thermal Annealing	23
4. Conclusion	27

References.....28

Summary.....32

Acknowledgement.....33



List of Figures

Figure 1. Structure of perovskite.....	2
Figure 2. Structure and photophysical properties of quasi-2D perovskite	6
Figure 3. Structure of perovskite LEDs.....	9
Figure 4. Working principles of perovskite LEDs.....	10
Figure 5. Structure of $\text{BA}_2\text{Cs}_{n-1}\text{Pb}_n\text{Br}_{3n+1}$ and perovskite LED device.....	16
Figure 6. Top view scanning electron microscope (SEM) images of the quasi-2D perovskite films with different thermal annealing conditions	17
Figure 8. Size distribution of grain in quasi-2D perovskite films with different thermal annealing conditions	19
Figure 9. The PL spectra of quasi-2D perovskite films with different thermal annealing conditions. Inset: Photograph of the films under UV.....	20
Figure 10. Comparative analysis of grain size and PL peak wavelength in quasi-2D perovskite films as a function of different thermal annealing	20
Figure 11. XRD and UV-vis absorption spectra of quasi-2D perovskite films with different thermal annealing conditions	21
Figure 12. Device performance of the quasi-2D perovskite LED with different thermal annealing conditions	24

List of Tables

Table 1. Detailed data about device performance of the quasi-2D perovskite

LED for each thermal annealing condition26



Crystallization Management with Tailored Thermal Annealing for Quasi-Two-Dimensional Perovskites Light-Emitting Diodes

Yeong Gyeong Kim

Department of Physics, The graduate School,
Pukyong National University

Abstract

Quasi-two dimensional (quasi-2D) perovskite has attracted considerable attention due to its large exciton binding energy and quantum confinement effect, which make it promising for use in light-emitting diodes (LEDs). However, quasi-2D perovskite films formed by solution processes suffer from inefficient energy transfer caused by undesired phase mixtures, poor crystallinity, and structural defects due to rapid crystal growth, leading to increased non-radiative recombination and reduced device performance. To minimize the defects in perovskite, the crystal growth of quasi-2D perovskite was adjusted by thermal annealing processes. Meanwhile, the grain size can be controlled by adjusting the annealing conditions, which allows for tuning the emission wavelength in the range of 507-519 nm. By optimizing the thermal annealing conditions, quasi-2D perovskite LEDs (PeLEDs) showed a maximum luminance of 4730 cd m⁻² and maximum external quantum efficiency of 15.5%, with an emission peak at 513 nm. The management of crystallization kinetics in quasi-2D perovskite promotes the practical application progress of PeLEDs.

1. Introduction

1.1. Perovskites

1.1.1 Metal Halide Perovskite Materials

Perovskite, a material class with a crystal structure like calcium titanate (CaTiO_3), was first discovered in Russia in 1839. These materials are commonly represented by the chemical formula ABX_3 .^[1] The conventional oxide-based perovskite consists of A as a divalent metal cation, B as a tetravalent metal cation, and X as a divalent oxygen anion.^[3] Recently, metal halide perovskite has gained prominence for their ease of fabrication and excellent optoelectronic properties. These consist of A as a monovalent organic or inorganic cation, B as a divalent metal cation, and X as a halogen anion replacing oxygen anion.^[4] Commonly, A is represented by a large monovalent cation such as cesium (Cs^+)^[5] and methylammonium (MA , CH_3NH_3^+).^[7] B by a divalent metal cation, like lead (Pb^{2+}) and tin (Sn^{2+})^[9], and X by halide ions including chloride (Cl^-), bromide (Br^-), and iodide (I^-).^[11]

Perovskite exhibits a cubic structure formed by the combination of three crystal structures: the simple cubic, body-centered cubic and face-centered cubic, as illustrated in figure 1.^[12] The structural stability of perovskite can be anticipated by the size ratios between the ions used at A, B, and X sites. These ratios can be quantified using the tolerance factor (t)^[13] and octahedral factor (μ)^[15], as proposed by Goldschmidt. The formulas for these factors are as follows:

$$t = \frac{r_A + r_X}{\sqrt{2}(r_B + r_X)}$$

$$\mu = \frac{r_B}{r_X}$$

In the equations, r_A , r_B , and r_X represent the effective ionic radii of A, B, and X ions, respectively. The cubic structure of perovskite informs prediction about its stability, with the t and μ playing key roles. The criteria for stability are defined as $0.85 < t < 1.1$ and $\mu > 0.44$, these values being inductively determined from studies on perovskite's structural characteristics.^[13]

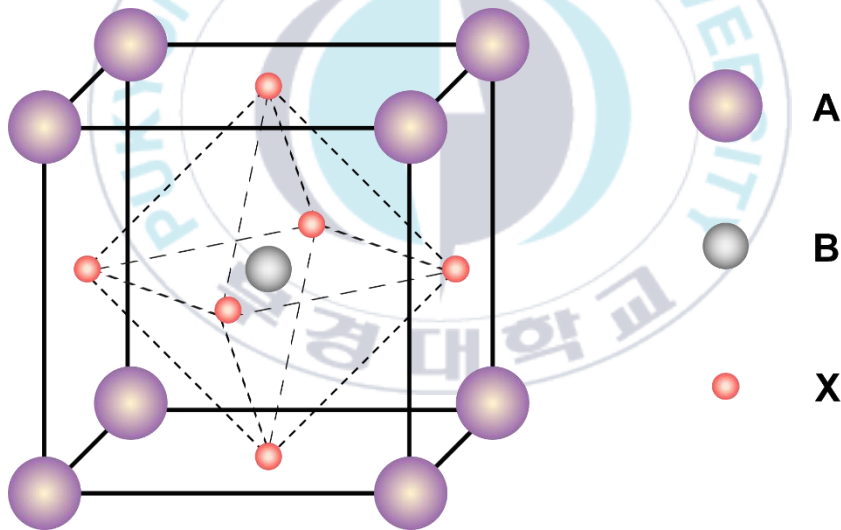


Figure 1. Structure of perovskite

Metal halide perovskites have a direct bandgap formed between the orbitals of the metal cation at the B site and the halogen anion at the X site. Unlike organic semiconductors with high exciton binding energies, excitons generated in metal halide perovskites can be separated easily by

thermal energy at room temperature due to their low exciton binding energy. A notable aspect of these perovskites is their defect tolerance, which can be attributed to the formation energies of defects. Defects that create deep-level states in the bandgap are less likely to be formed due to their high formation energy in metal halide perovskites. Conversely, defects with low formation energy create shallow level states which do not significantly impact the electronic properties of the material.^[17]

The research achievements in the study of metal halide perovskites for solar cells, with their process advantages and excellent optoelectronic properties, have led to active research in the field of light-emitting devices. In terms of the characteristics related to luminescence in metal halide perovskites, the overlap of the orbitals of B-site and X-site ions determining the bandgap is related to the perovskite structure.^[19]

The bandgap of metal halide perovskites can be adjusted from the near-infrared to the entire visible spectrum by changing and modifying the composition of B-site metal cations and X-site halide ions. Additionally, the adjustment of the structural stability of perovskite crystals through A-site ions can further improve the luminescent properties. This versatility makes metal halide perovskites an attractive material for display applications requiring high color reproducibility in a wide range of natural colors.

However, the low exciton binding energy and changes in the structural stability of the crystal with different composition highlight the need for continued research in the field of perovskite as a luminescence material

for display.

1.1.2 Qausi-2D Perovskite Materials

Perovskites can be controlled across various dimensions, ranging from zero-dimensional quantum dots to three-dimensional (3D) bulk states. Typically, perovskite films for device fabrication are grown by promoting the binding of ions in solution or at the interfaces of touching thin films. The 3D bulk perovskite suffers from hindered radiative recombination due to its low exciton binding energy.^[22] Additionally, defects easily formed at particle boundaries (dangling bonds) create deep-level states in bandgap, inducing non-radiative recombination and significantly reducing the efficiency of light-emitting diodes in the field.^[23]

To address this, researchers have focused on reducing the dimensionality to enhance quantum confinement effects and, simultaneously, increase exciton binding energy, promoting a higher radiative recombination rate for improved quantum yield. Quasi-two-dimensional perovskites (quasi-2D perovskites) represent a 2D perovskite structure demonstrating strong quantum confinement effects compared to 3D perovskites.^[24] Additional organic ligands introduced for the formation of 2D perovskite effectively reduce the formation of dangling bond defects at the boundaries. Moreover, the fabrication process is simplified using conventional low-temperature solution processes. Quasi-2D perovskites possess a layered structure represented by the chemical formula $L_2A_{n-1}B_nX_{3n+1}$, where L typically represents organic spacer like butylammonium

(BA), and n indicates the number of perovskite octahedral units $[\text{BX}_6]^{4-}$ between the two organic spacer layers. By adjusting the organic spacers, the number of layers in quasi-2D perovskites can be controlled, enabling tuning of the emission wavelength even with the same material.^[25] However, the application of quasi-2D perovskites in light-emitting devices faces challenges due to increased electrical resistance caused by insulating organic spacers.

As illustrated in figure 2, the organic spacer separates the 3D perovskite to the 2D perovskite layers, creating a structure where the organic spacer layer acts as a barrier, and the perovskite layer serves as a quantum well.^[27] This design enhances the quantum confinement effect, leading to an increase in exciton binding energy. The value of n determines the quantum confinement effect, with lower values leading to increased quantum confinement and a blue-shifted emission wavelength.

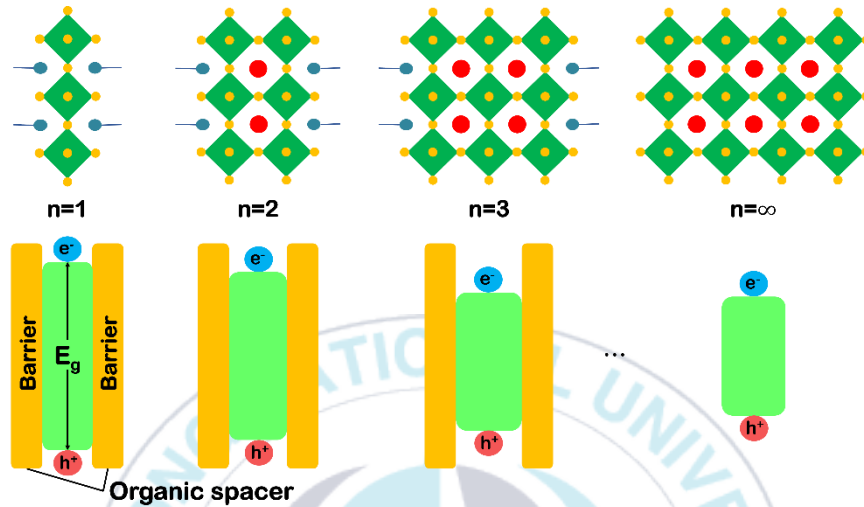


Figure 2. Structure and photophysical properties of quasi-2D perovskite

Quasi-2D perovskites film can be easily formed through one-step solution processing and low-temperature thermal annealing in LED fabrication due to their self-assembling multiple quantum well structures.^[29] But the distribution of n in quasi-2D perovskite film is not uniform due to low energetical difference in formation with short film formation time. By having the mixed phase (mixture of quasi-2D perovskite with different n), the energy funneling occurs in quasi-2D perovskite film and facilitates easy charge accumulation at larger n phase leading to more efficient charge carrier recombination in perovskite.^[30]

1.1.3. Quasi-2D Perovskite for Light-Emitting Diodes

Perovskites offer some advantages, such as tunable wavelength, high PLQY, and wide color gamut. In perovskite light-emitting diodes (PeLEDs), a variety of perovskite materials are utilized in the emissive layer, ranging from low-dimensional forms to bulk configurations. PeLEDs have achieved external quantum efficiencies (EQEs) exceeding 20% in the red and green spectral regions.^[31] The PeLEDs signifies their promising potential in next generation displays and optical communication applications.

Quasi-2D perovskites, with their unique structure, offer advantages, such as high radiative recombination rate and smooth energy transfer, in thin film formation for device applications compared to traditional 3D bulk perovskites. The transition involves optimizing deposition techniques, adjusting composition and phase-distribution, and addressing challenges related to stability and interface engineering. Researchers have explored solution-based methods for efficient thin film deposition and have focused on interface engineering to enhance charge transport and reduce recombination at interfaces.^[32] The role of organic ligands in tuning electronic properties and strategies for achieving long-term stability in thin devices have also been investigated.^[34] The ongoing research aims to unlock the full potential of quasi-2D perovskites in practical device applications.

1.1.4. Research Background

Recently, rapid advancements have been made in the development of perovskite LEDs. This progress serves as a foundation for perovskite's role as an emissive material in next-generation ultra-high-definition display technologies. Perovskite, especially in quasi-2D form, offers the advantage of easily tuning the emission wavelength by adjusting the internal material composition or ratio.^[35] It exhibits a narrow full-width at half-maximum (FWHM) for emission wavelengths, ensuring high color purity, and boasts a high photoluminescence quantum yield (PLQY), making it a promising emissive material.

Quasi-2D perovskite, with its strong quantum confinement effects due to its quantum well structure, has been a subject of extensive research. The fabrication of quasi-2D perovskite involves a one-step solution process, combining [AX] and [BX₂] materials, along with organic spacers, dissolved in a polar organic solvent like dimethylsulfoxide (DMSO).^[37] The resulting solution is coated onto a substrate and undergoes a thermal annealing process to facilitate the growth of quasi-2D perovskite. While this fabrication process is simple and cost-effective, the rapid crystallization during the thermal annealing process will induce defects such as surface imperfections and unstable crystal growth, leading to non-radiative exciton recombination and performance degradation.

To address these issues, this study focuses on controlling the growth of quasi-2D perovskite crystals by adjusting the thermal annealing conditions. The goal is to minimize defect formation during the fabrication

process. Additionally, the study optimized the thermal annealing condition for more efficient quasi-2D perovskite, providing insights for future research in this field.

1.2. Light-Emitting Diodes

1.2.1 Working Principle of Light-Emitting Diodes

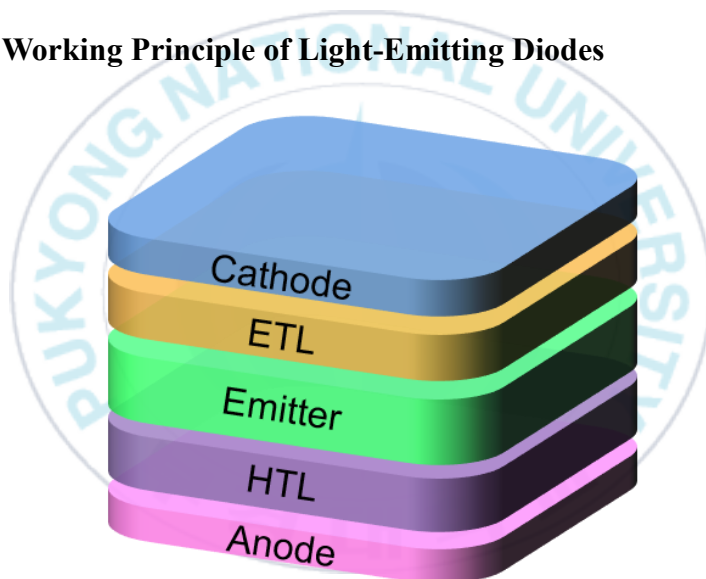


Figure 3. Structure of perovskite LEDs

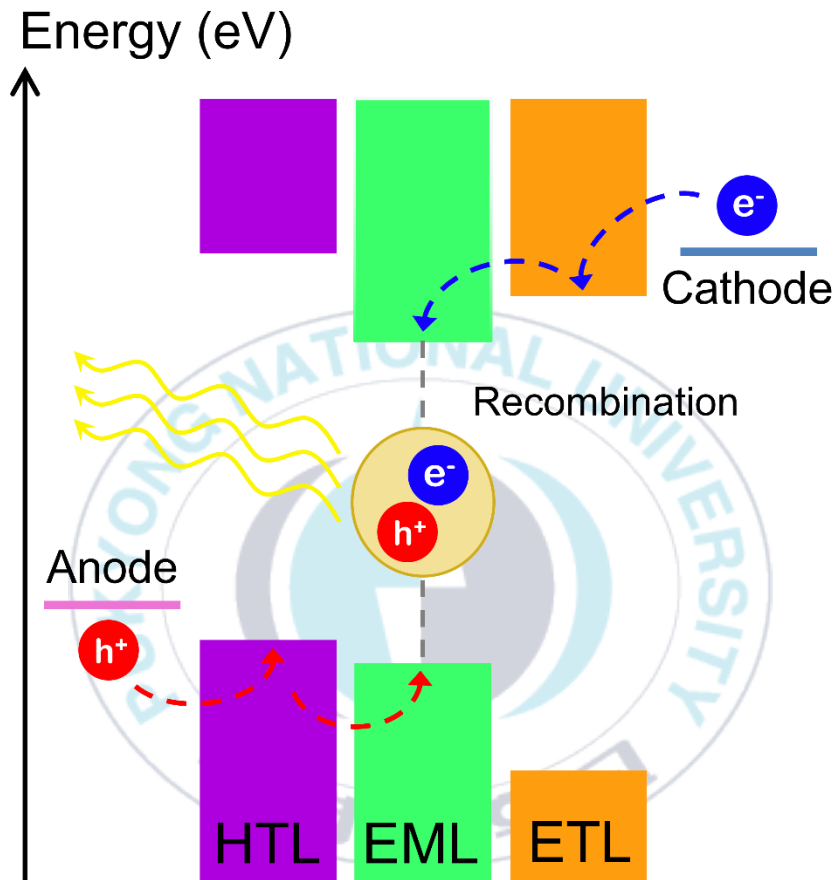


Figure 4. Working principles of perovskite LEDs

Perovskite LEDs with the structure shown in figure 3 operate based on the following principles:

- (1) When current flows through each electrode of the perovskite LED, electrons and holes move to the electron transport layer (ETL) and hole transport layer (HTL), respectively. Electrons

are injected into the lowest unoccupied molecular orbital (LUMO) of the ETL, while holes are injected into the highest occupied molecular orbital (HOMO) of the HTL. To enhance the overall efficiency of the LED, smooth and balanced injection of electrons and holes is crucial, requiring alignment of the energy levels of the ETL and HTL.

- (2) Electrons and holes injected into the ETL and HTL, respectively, are further injected into the emission layer (EML). In the EML, recombination of electrons and holes occurs through Coulomb forces, forming excitons and releasing energy in the form of light. However, factors such as non-radiative exciton recombination due to traps at the interfaces of EML-ETL and EML-HTL, as well as non-radiative exciton recombination within the perovskite and appropriately aligning the energy levels of the EML are crucial for addressing these issues.

Excitons form in a 1:3 ratio of singlet and triplet states. Singlet excitons have a very short lifetime of approximately 10^{-9} seconds, while triplet excitons have a relatively longer lifetime of around 10^{-6} seconds. The fluorescent materials only release photons through singlet excitons transition. On the other hand, the phosphorescent materials can use all excitons, offering a theoretical internal quantum efficiency of 100%.^[38]

1.2.2 Characteristics of Light-Emitting Diodes

For achieving high-performance perovskite LEDs, as mentioned earlier, the choice of ETL and HTL is crucial. These layers facilitate smooth and balanced injection of charges into the EML. When selecting suitable ETL and HTL for perovskite LEDs, key considerations include ensuring low charge injection barriers to facilitate charge transport, while simultaneously establishing sufficiently high barriers to block the injection of opposite charges and maintaining high charge carrier mobility.^[39] Minimizing non-radiative recombination at the interface between the transport layer and EML is essential. Additionally, for efficient light-emitting devices, optimizing film morphology and crystal characteristics through controlled crystal growth during the formation of quasi-2D perovskites, adjusting the distribution of crystal sizes, and optimizing electrical properties through n-distribution control in quasi-2D perovskite films are necessary. This optimization enables effective charge injection and recombination, achieving the desired color emission tailored to the wavelength of light.

The point at which light emission begins or the voltage at the current density where light emission starts is referred to as the turn-on voltage. The minimum energy required for charge injection starts from the voltage corresponding to the energy bandgap of the EML. The turn-on voltage increases when the injection barriers of each transport layer are high or when the charge mobility is unbalanced.

In the analysis of the characteristics of PeLEDs, current efficiency (CE), and EQE represent different aspects of the LED's performance.^[41]

(1) Current Efficiency (CE):

CE indicates how effectively current is converted into photons. It represents the ratio of the amount of light generated to the given current.

$$\begin{aligned} \text{current efficiency (cd A}^{-1}\text{)} \\ &= \frac{\text{Luminance (cd m}^{-2}\text{)}}{\text{Current density (mA cm}^{-2}\text{)}} \times 10^{-1} \end{aligned}$$

(2) External Quantum Efficiency (EQE):

EQE indicates the ratio of the number of photons emitted externally to the number of electron-hole pairs injected into the LED. It quantifies how effectively photons are generated externally.

$$\begin{aligned} \text{external quantum efficiency (\%)} \\ &= \frac{\text{The number of emitted photons}}{\text{The number of injected electrons}} \\ &\quad \times 100 \end{aligned}$$

These characteristics are used to evaluate the efficiency and performance of the LED. Considering these characteristics together provides a comprehensive evaluation of the LED's overall performance.

2. Experimental Section

2.1 Materials

Cesium bromide (99.9%), Lead Bromide (99.9%), Butyl ammonium (99.9%), Dimethylsulfoxide (DMSO; 99.9%), 1,4,7,10,13,16-Hexaoxacyclooctadecane (18-crown-6; 99%), Poly(9-vinylcabazole) (PVK; powder, $M_w \sim 1,100,000$), Chlorobenzene (CB; 99.8%) was purchased from Sigma Aldrich. Aqueous solution of Poly(3,4-ethylenedioxythiophene)polystyrene sulfonate (PEDOT:PSS; Clevis Al 4083) was acquired from Heraeus. 2,2',2''-(1,3,5-benzinetriyl)tris(1-phenyl-1-H-benzimidazole) (TPBi; 99.9%) was acquired from OSM. LiF (99.9%), Al (99.9%) was purchased from iTASCO.

2.2 Device Fabrication

After preparing a solution of 18-crown-6 in DMSO with a concentration of 4 mg/ml, a mixture containing BABr (22.5 mg, 0.14 mol), CsBr (30.7 mg, 0.14 mol) PbBr₂ (52.8 mg, 0.14 mol) was combined in a single container with 1 ml of the prepared 18-crown-6 in DMSO solution. The entire process was carried out in a nitrogen (N₂) gas environment while utilizing a stirring bar. The mixture was stirred at 60°C for 1 hour, resulting in the formation of a perovskite solution, specifically BA₂Cs_{n-1}Pb_nBr_{3n+1}.

To create a perovskite LED device, the process involves treating a glass/ITO substrate with oxygen plasma for 20 minutes to modify the ITO surface to hydrophilic. Subsequently, a PEDOT:PSS solution is spin-coated onto the ITO surface at 4500 rpm for 40 seconds. Immediately after,

a thermal annealing is conducted at 150°C for 10 minutes to remove moisture contained in PEDOT:PSS. Next, in a N₂ gas environment, PVK (4 mg/ml in CB) is spin-coated onto the PEDOT:PSS layer at 4000 rpm for 40 seconds, forming the HTL. A subsequent thermal annealing is performed at 130°C for 10 minutes.

Following this, the BA₂Cs_{n-1}Pb_nBr_{3n+1} solution is spin-coated onto the HTL at 500 rpm for 5 seconds, followed by continuous spin-coating at 5000 rpm for 40 seconds. The process then undergoes thermal annealing step using an encapsulation growth method for controlling the crystal growth rate of perovskite.^[42] For the ETL, thermal vacuum deposition is conducted under a high vacuum condition of 1×10⁻⁶ Torr. The ETL deposition involves TPBi (70 nm), LiF (2 nm), and Al (100 nm).

3. Result and Discussion

3.1 Device Structure of Quasi-2D Perovskite Light-Emitting Diodes

In this study, we adopted and utilized quasi-2D perovskite $\text{BA}_2\text{Cs}_{n-1}\text{Pb}_n\text{Br}_{3n+1}$. Figure 5 illustrates the structure of the prepared perovskite LED device for this paper.

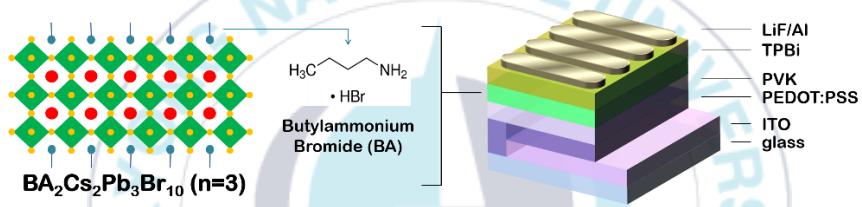


Figure 5. Structure of $\text{BA}_2\text{Cs}_{n-1}\text{Pb}_n\text{Br}_{3n+1}$ and perovskite LED device

The left diagram shows a schematic illustration of the layer structure of $\text{BA}_2\text{Cs}_{n-1}\text{Pb}_n\text{Br}_{3n+1}$ quasi-2D perovskite when $n=3$, along with the structure of BA. The right diagram illustrates the overall structure of the perovskite LED device.

3.2 Characteristics of Quasi-2D Perovskite Films with Thermal Annealing

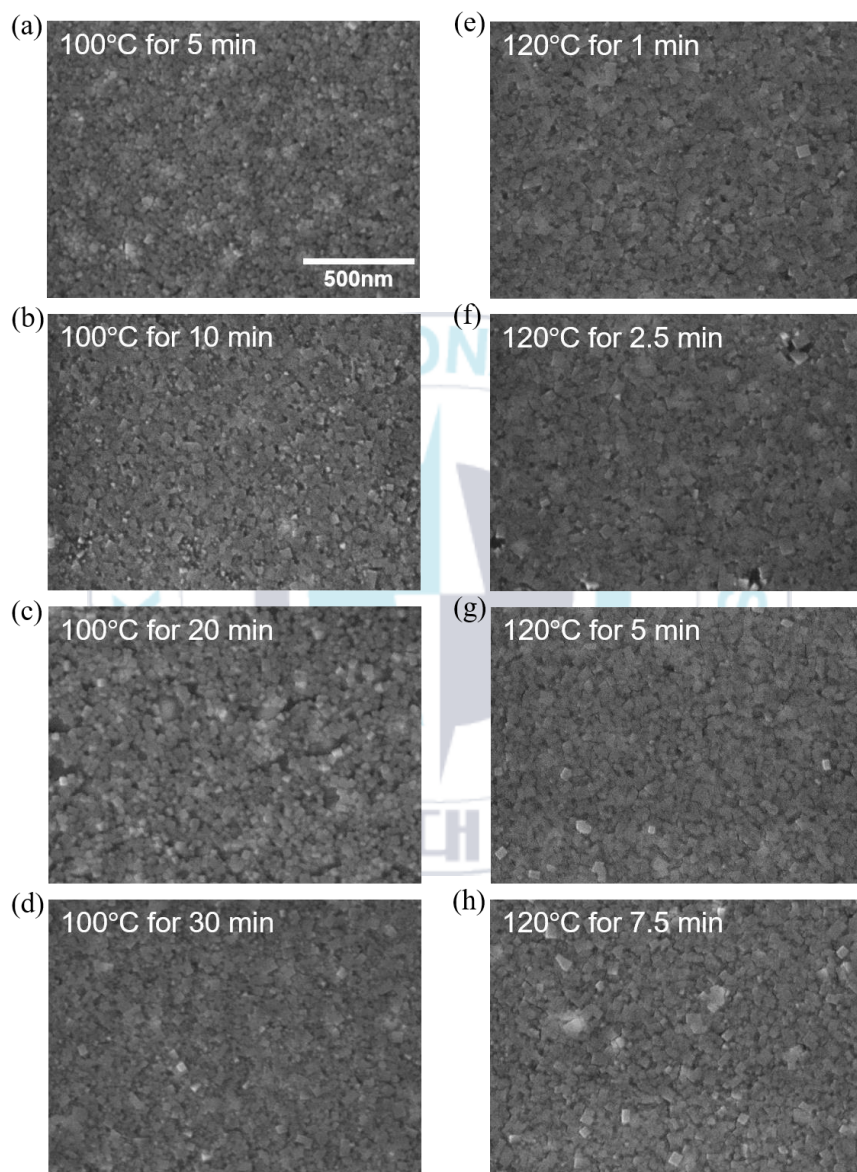


Figure 6. Top view scanning electron microscope (SEM) images of the quasi-2D perovskite films with different thermal annealing conditions

The thermal annealing condition for the original quasi-2D perovskite $\text{BA}_2\text{Cs}_{n-1}\text{Pb}_n\text{Br}_{3n+1}$ was 100°C for 5 minutes. To investigate the changes on the perovskite surface with increasing thermal annealing time, the surfaces were analyzed using scanning electron microscopy (SEM) at 5-minute intervals (Figure 6a-d). In figure 6, it can be observed that the grain size increases with the prolonged thermal annealing process. Particularly, after thermal annealing for 20 minutes, excessive thermal annealing led to the formation of pinholes and defects (Figure 6c), and after thermal annealing for 30 minutes, aggregation occurred due to excessive thermal annealing, causing deterioration of crystallinity (Figure 6d). This significantly compromised the surface crystallinity and uniformity of the crystals. Although the thermal annealing process contributes to the crystalline growth of quasi-2D perovskite, excessive thermal annealing adversely affected the material due to its vulnerability to temperature.

To observe the changes at a higher temperature, experiments were conducted at 120°C (Figure 6e-f). The thermal annealing time was adjusted accordingly due to the higher temperature. Similar results were obtained at 120°C , where an increase in grain size was observed with prolonged thermal annealing time. After thermal annealing for 7.5 minutes at 120°C , excessive thermal annealing also resulted in a deterioration of crystallinity. Detailed values for grain size are provided in figure 7.

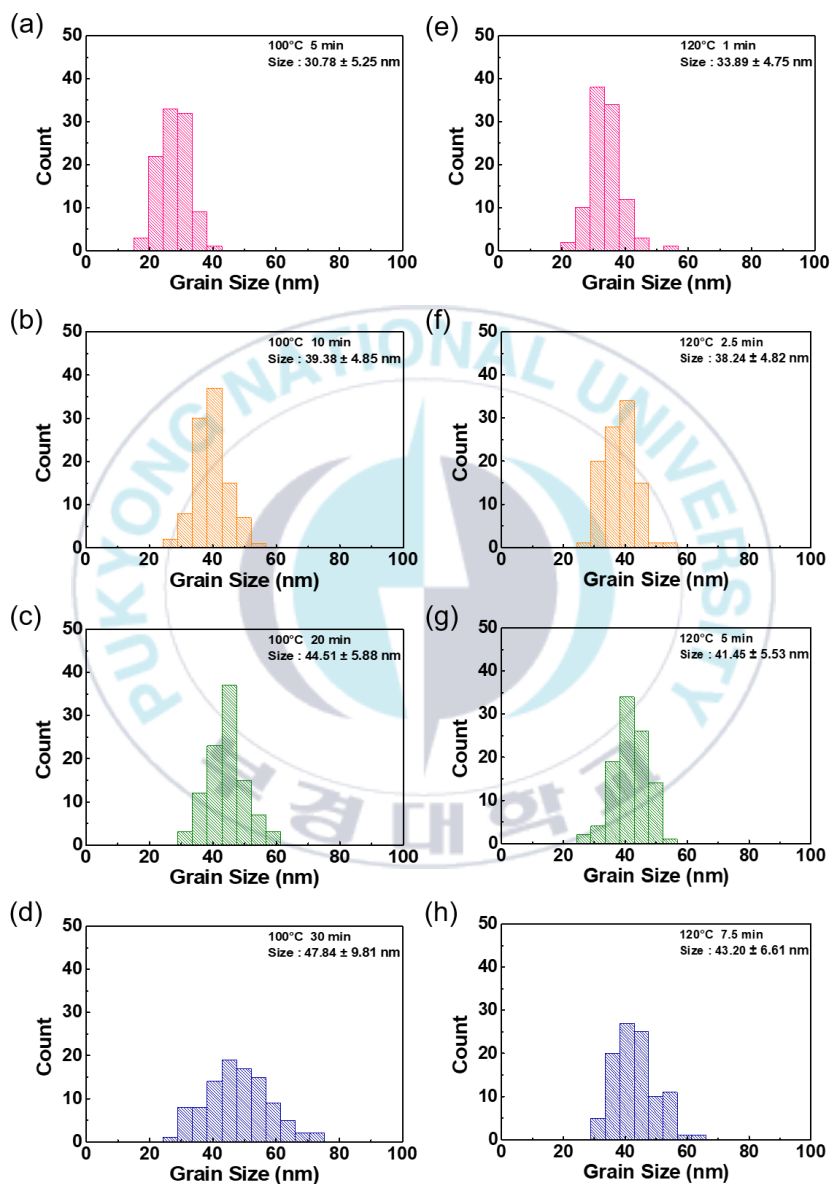


Figure 7. Size distribution of grain in quasi-2D perovskite films with different thermal annealing conditions

Figure 8 depicts the photoluminescence (PL) spectra of the perovskite films with different thermal annealing conditions. Through this, the redshift in the PL spectra was observed with increasing thermal annealing time. This observation correlated with the increase in grain size depicted in figure 7.

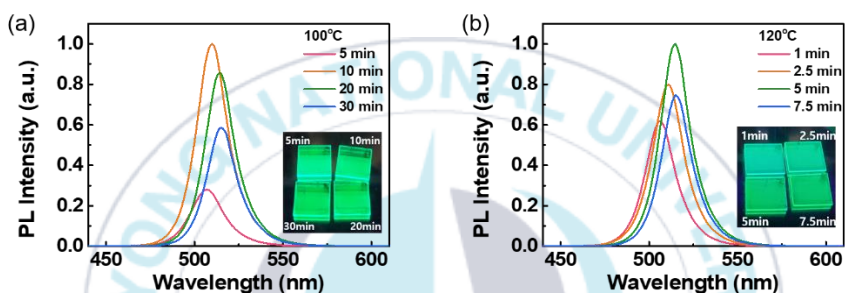


Figure 8. The PL spectra of quasi-2D perovskite films with different thermal annealing conditions. Inset: Photograph of the films under UV

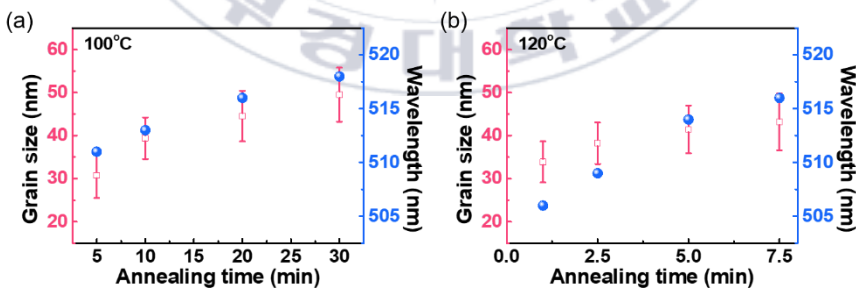


Figure 9. Comparative analysis of grain size and PL peak wavelength in quasi-2D perovskite films as a function of different thermal annealing

The occurrence of a redshift in the wavelength as the grain size increases is evident. Through this observation, it can be concluded that the

increase in grain size in quasi-2D perovskite corresponds to an increase in the n-value. Therefore, the prolonged thermal annealing process led to an overall increase in the average n-value in quasi-2D perovskite, resulting in the observed redshift in the PL wavelength.

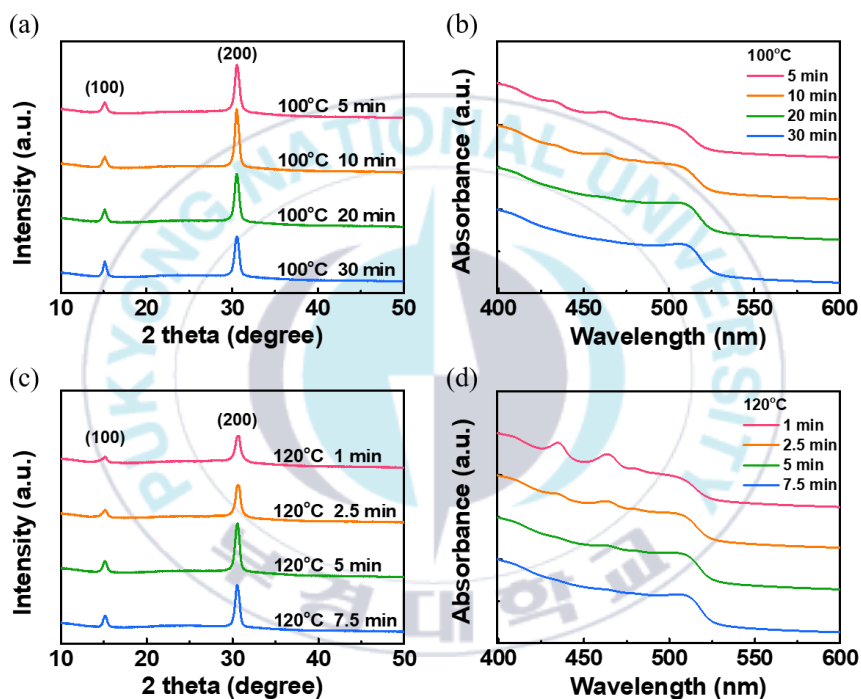


Figure 10. XRD and UV-vis absorption spectra of quasi-2D perovskite films with different thermal annealing conditions

Figure 10 illustrates the crystal structure and optical characteristics of the quasi-2D perovskite film with increasing thermal annealing time. In figure 10a, the X-ray diffraction (XRD) patterns of the perovskite film are observed, revealing peaks corresponding to (100) at a diffraction angle of 15.1° and (200) at 30.5° throughout. When the thermal annealing time is

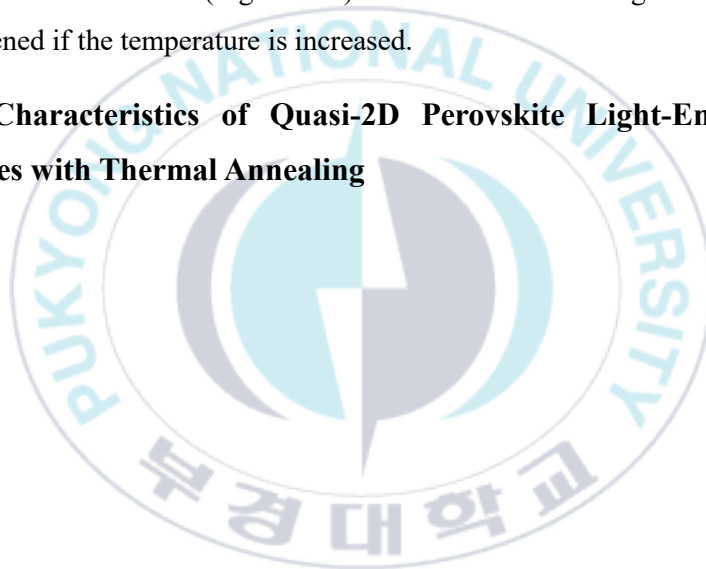
increased from 5 to 10 minutes at 100°C, the intensities of both (100) and (200) peaks increase, indicating that a 10-minute thermal annealing time is optimal for the crystal growth of quasi-2D perovskite at 100°C temperature. Conversely, for thermal annealing times of 20 minutes and beyond, the peak intensities decrease due to defects affecting crystallinity and uniformity. This suggests that a 10-minute thermal annealing process at 100°C provided optimal energy for effective crystal growth, while longer durations or excessive thermal annealing led to a decrease in peak intensity due to issues such as crystal deformation.

Similar observations were made for thermal annealing at 120°C, with the strongest XRD peak observed after a 5-minute thermal annealing process (Figure 10c). In figure 10b, the UV-vis absorption spectrum of the perovskite film with increasing thermal annealing time at 100°C is presented. The comparison of absorption peak intensities at different positions allows the observation of the distribution of n-values in quasi-2D perovskite. As the thermal annealing time increases, the intensity of peaks corresponding to lower n-values decreases, while those corresponding to higher n-values increase. This supports the earlier explanation that an increase in thermal annealing time at the same temperature corresponds to an increase in n-values. For a 5-minute thermal annealing time, absorption peaks corresponding to $n=1, 2,$ and 3 are observed at 405, 435, and 464 nm, respectively. As the thermal annealing time increases, the intensity of these peaks gradually decreases, and absorption peaks corresponding to higher n-values emerge at 505 nm (Figure 10b). This indicates that the composition of n-values in quasi-2D

perovskite changes with thermal annealing conditions. The amount of small n-phase decreases with the annealing temperature increased, demonstrating that the phase distribution can be optimized by thermal annealing.

Similar trends in the increase of n-values with thermal annealing time are observed at 120°C (Figure 10d). It shows that annealing time can be shortened if the temperature is increased.

3.3 Characteristics of Quasi-2D Perovskite Light-Emitting Diodes with Thermal Annealing



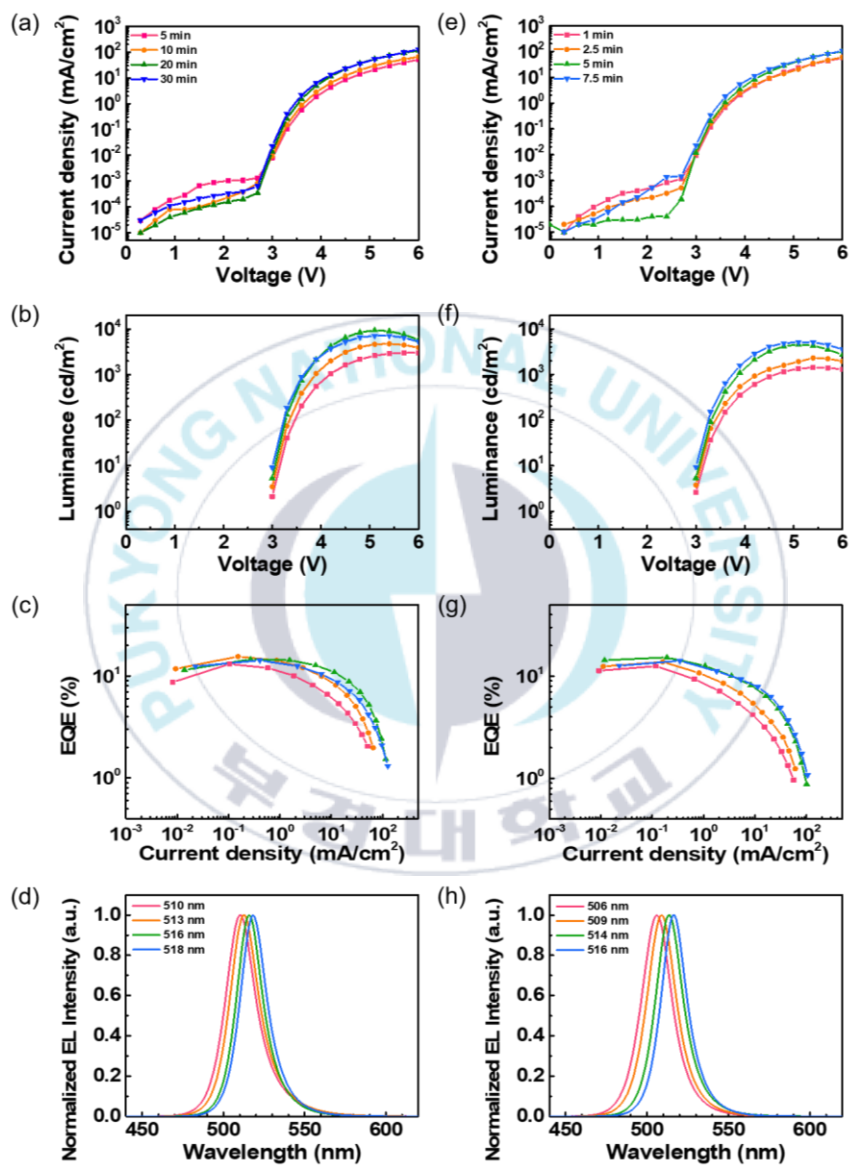


Figure 11. Device performance of the quasi-2D perovskite LED with different thermal annealing conditions

In figure 11a-d, the device performance of the PeLED treated with thermal annealing at 100°C is presented. Figure 11a-b shows the graph of current density and luminance as a function of voltage. It can be observed that the amount of injected current density increases with the increase in thermal annealing time. This is attributed to the larger grain size as the thermal annealing time increases, leading to a higher average n-value in quasi-2D perovskite. The increase in current density is accompanied by an increase in luminance, reaching up to 9380 cd m⁻², compared to the value of 3002 cd m⁻² with thermal annealing time of 5 minutes (Figure 11b). However, for a thermal annealing time of 30 minutes, the luminance value decreases. This is attributed to the deteriorating effect on crystallinity outweighing the increase in luminance due to increased current. The EQE improves, reaching 15.5 % for the device treated with thermal annealing at 100°C for 10 minutes, compared to the initial value of 13.1% (Figure 11c). Figure 11d presents the normalized electroluminescence (EL) spectra of PeLED with different thermal annealing conditions. As thermal annealing time increases, the emission wavelength shifts from the initial 511 nm to 518 nm, indicating a redshift.

Similar trends are observed for the case where thermal annealing is conducted at 120°C (Figure 11e-h). Particularly, the results for thermal annealing at 120°C for 5 minutes and at 100°C for 10 minutes show similar characteristics. The EQE for thermal annealing at 120°C for 5 minutes is 15.3%, comparable to the value of 15.5 % for thermal annealing at 100°C for 10 minutes. This suggests that the extent of crystalline growth and device performance for quasi-2D perovskite is similar for these two

thermal annealing conditions. Detailed data for each LED device performance is provided in Table 1.

(a)

Annealing time at 100 °C	L_{max} [cd/m ²] @ bias [V]	LE_{max} [cd/A] @ bias [V]	EQE_{max} [%] @ bias [V]	Turn-on Voltage [V] @ 0.1cd/m ²	Wavelength [nm]	FWHM [nm]
5 min	3002@5.7	39.36@3.3	13.10@3.3	3.0	511	21
10 min	4730@5.4	48.80@3.3	15.52@3.3	3.0	513	21
20 min	9380@5.1	49.11@3.3	14.58@3.3	3.0	516	19
30 min	7109@5.4	46.04@3.3	14.25@3.3	3.0	518	19

(b)

Annealing time at 120 °C	L_{max} [cd/m ²] @ bias [V]	LE_{max} [cd/A] @ bias [V]	EQE_{max} [%] @ bias [V]	Turn-on Voltage [V] @ 0.1cd/m ²	Wavelength [nm]	FWHM [nm]
1 min	1423@5.4	30.88@3.3	12.54@3.3	3.0	506	22
2.5 min	2307@5.4	41.10@3.3	13.80@3.3	3.0	510	21
5 min	4578@5.1	47.27@3.3	15.30@3.3	3.0	514	20
7.5 min	5153@5.1	43.59@3.3	14.17@3.3	3.0	516	19

Table 1. Detailed data about device performance of the quasi-2D perovskite LED for each thermal annealing condition

4. Conclusion

In conclusion, the crystal growth of quasi-2D perovskites can be effectively controlled by using thermal annealing engineering, which results in reduced perovskite defects and improved device stability. In this paper, the variations in crystalline growth according to thermal annealing conditions were investigated, identifying the optimal conditions for crystallization and revealing that excessive thermal annealing could actually impair crystallinity. And the relationship between thermal annealing conditions and the n-phase distribution in quasi-2D perovskite was explored by UV-vis spectrum. Furthermore, the optimal thermal annealing conditions were identified for enhancing the device performance of quasi-2D perovskite. The device performance is enhanced by 15.5 % and 15.3 % EQEs for annealing 100°C for 10 minute and 120°C for 5 minute respectively. And the device performance shows low damage at 100°C for 20 minute and maximum optical intensity was achieved by reducing small n phase in perovskite. These results provide insights into the optimization of thermal annealing processes for future quasi-2D perovskite research, contributing to the advancement of this field.

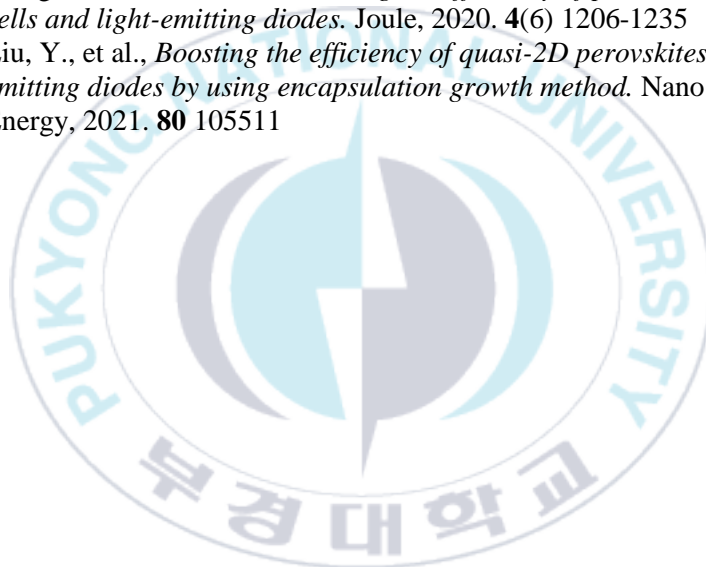
References

- [1] Sahu, S.K., P.S. Maram, and A. Navrotsky, *Thermodynamics of nanoscale calcium and strontium titanate perovskites*. Journal of the American Ceramic Society, 2013. **96**(11) 3670-3676
- [2] Attfield, J.P., P. Lightfoot, and R.E. Morris, *Perovskites*. Dalton Transactions, 2015. **44**(23) 10541-10542
- [3] Kumar, A., A. Kumar, and V. Krishnan, *Perovskite oxide based materials for energy and environment-oriented photocatalysis*. Acs catalysis, 2020. **10**(17) 10253-10315
- [4] Leijtens, T., et al., *Stability of metal halide perovskite solar cells*. Advanced Energy Materials, 2015. **5**(20) 1500963
- [5] Song, J., et al., *Quantum dot light-emitting diodes based on inorganic perovskite cesium lead halides (CsPbX₃)*. Advanced materials, 2015. **27**(44) 7162-7167
- [6] Bekenstein, Y., et al., *Highly luminescent colloidal nanoplates of perovskite cesium lead halide and their oriented assemblies*. Journal of the American Chemical Society, 2015. **137**(51) 16008-16011
- [7] Leguy, A.M., et al., *The dynamics of methylammonium ions in hybrid organic–inorganic perovskite solar cells*. Nature communications, 2015. **6**(1) 7124
- [8] Kim, J., et al., *The role of intrinsic defects in methylammonium lead iodide perovskite*. The journal of physical chemistry letters, 2014. **5**(8) 1312-1317
- [9] Liu, X., et al., *Solvent engineering improves efficiency of lead-free tin-based hybrid perovskite solar cells beyond 9%*. ACS Energy Letters, 2018. **3**(11) 2701-2707
- [10] Nishimura, K., et al., *Lead-free tin-halide perovskite solar cells with 13% efficiency*. Nano Energy, 2020. **74** 104858
- [11] Lin, K., et al., *Perovskite light-emitting diodes with external quantum efficiency exceeding 20 per cent*. Nature, 2018. **562**(7726) 245-248
- [12] Akhade, S.A. and J.R. Kitchin, *Effects of strain, d-band filling, and oxidation state on the bulk electronic structure of cubic 3d perovskites*. The Journal of chemical physics, 2011. **135**(10)
- [13] Li, Z., et al., *Stabilizing perovskite structures by tuning tolerance factor: formation of formamidinium and cesium lead iodide solid-state alloys*. Chemistry of Materials, 2016. **28**(1) 284-292

- [14] Tidrow, S.C., *Mapping comparison of Goldschmidt's tolerance factor with Perovskite structural conditions*. *Ferroelectrics*, 2014. **470**(1) 13-27
- [15] Bartel, C.J., et al., *New tolerance factor to predict the stability of perovskite oxides and halides*. *Science advances*, 2019. **5**(2) eaav0693
- [16] Ji, D., et al., *Regulatory tolerance and octahedral factors by using vacancy in APbI3 perovskites*. *Vacuum*, 2019. **164** 186-193
- [17] Cho, S.H., et al., *Investigation of defect-tolerant perovskite solar cells with long-term stability via controlling the self-doping effect*. *Advanced Energy Materials*, 2021. **11**(17) 2100555
- [18] Zhang, J., Y. Zhong, and G. Li, *Benign Deep-Level Defects in Cesium Lead Iodine Perovskite*. *The Journal of Physical Chemistry C*, 2021. **125**(48) 27016-27022
- [19] Xue, J., et al., *Reconfiguring the band-edge states of photovoltaic perovskites by conjugated organic cations*. *Science*, 2021. **371**(6529) 636-640
- [20] Tang, G., P. Ghosez, and J. Hong, *Band-edge orbital engineering of perovskite semiconductors for optoelectronic applications*. *The Journal of Physical Chemistry Letters*, 2021. **12**(17) 4227-4239
- [21] Slavney, A.H., et al., *A pencil-and-paper method for elucidating halide double perovskite band structures*. *Chemical science*, 2019. **10**(48) 11041-11053
- [22] Wang, Q., et al., *Quantum confinement effect and exciton binding energy of layered perovskite nanoplatelets*. *Aip Advances*, 2018. **8**(2)
- [23] Du, Y., et al., *Manipulating the Formation of 2D/3D Heterostructure in Stable High-Performance Printable CsPbI3 Perovskite Solar Cells*. *Advanced Materials*, 2023. **35**(5) 2206451
- [24] Chakraborty, R., G. Paul, and A.J. Pal, *Quantum Confinement and Dielectric Deconfinement in Quasi-Two-Dimensional Perovskites: Their Roles in Light-Emitting Diodes*. *Physical Review Applied*, 2022. **17**(5) 054045
- [25] Li, D., et al., *Spontaneous Formation of Upper Gradient 2D Structure for Efficient and Stable Quasi-2D Perovskites*. *Advanced Materials*, 2021. **33**(34) 2101823
- [26] Sheng, X., et al., *Quasi-2D halide perovskite crystals and their optoelectronic applications*. *Journal of Materials Chemistry A*,

2022. **10**(37) 19169-19183
- [27] Liang, J., et al., *A finely regulated quantum well structure in quasi-2D Ruddlesden–Popper perovskite solar cells with efficiency exceeding 20%*. Energy & Environmental Science, 2022. **15**(1) 296-310
- [28] Wang, K., et al., *Two-dimensional halide perovskite quantum-well emitters: A critical review*. EcoMat, 2021. **3**(3) e12104
- [29] Fu, Y., et al., *Engineering of annealing and surface passivation toward efficient and stable quasi-2d perovskite light-emitting diodes*. The Journal of Physical Chemistry Letters, 2021. **12**(48) 11645-11651
- [30] Jiang, Y., J. Wei, and M. Yuan, *Energy-funneling process in quasi-2D perovskite light-emitting diodes*. The Journal of Physical Chemistry Letters, 2021. **12**(10) 2593-2606
- [31] Liu, Z., et al., *Perovskite light-emitting diodes with EQE exceeding 28% through a synergetic dual-additive strategy for defect passivation and nanostructure regulation*. Advanced Materials, 2021. **33**(43) 2103268
- [32] Lin, Y.K., et al., *Realizing High Brightness Quasi-2D Perovskite Light-Emitting Diodes with Reduced Efficiency Roll-Off via Multifunctional Interface Engineering*. Advanced Science, 2023. **10**(26) 2302232
- [33] Yan, L., et al., *Charge-carrier transport in quasi-2D Ruddlesden–Popper perovskite solar cells*. Advanced Materials, 2022. **34**(7) 2106822
- [34] Fu, W., et al., *Tailoring the functionality of organic spacer cations for efficient and stable quasi-2D perovskite solar cells*. Advanced Functional Materials, 2019. **29**(25) 1900221
- [35] Yuan, S., et al., *Optimization of low-dimensional components of quasi-2D perovskite films for deep-blue light-emitting diodes*. Advanced Materials, 2019. **31**(44) 1904319
- [36] Kumar, G.S., R.R. Sumukam, and B. Murali, *Quasi-2D perovskite emitters: a boon for efficient blue light-emitting diodes*. Journal of Materials Chemistry C, 2020. **8**(41) 14334-14347
- [37] Kim, J.Y., et al., *Phase Behavior of Quasi-2D Hybrid Lead Bromide Perovskite Precursor Solutions*. ACS Applied Optical Materials, 2023
- [38] Qin, C., et al., *Triplet management for efficient perovskite light-*

- emitting diodes*. Nature Photonics, 2020. **14**(2) 70-75
- [39] Ollearo, R., et al., *Ultralow dark current in near-infrared perovskite photodiodes by reducing charge injection and interfacial charge generation*. Nature Communications, 2021. **12**(1) 7277
- [40] Zhang, T., et al., *Green perovskite light-emitting diodes with simultaneous high luminance and quantum efficiency through charge injection engineering*. Science Bulletin, 2020. **65**(21) 1832-1839
- [41] Jeong, S.-H., et al., *Characterizing the efficiency of perovskite solar cells and light-emitting diodes*. Joule, 2020. **4**(6) 1206-1235
- [42] Liu, Y., et al., *Boosting the efficiency of quasi-2D perovskites light-emitting diodes by using encapsulation growth method*. Nano Energy, 2021. **80** 105511



Summary

준 2차원 페로브스카이트는 큰 여기자 결합 에너지와 양자 구속 효과로 인해 상당한 주목을 받아왔으며, 이는 차세대 발광 다이오드의 소재로 각광을 받고 있습니다. 그러나 용액 공정으로 형성된 준 2차원 페로브스카이트 필름은 좋지 않은 상의 혼합으로 인해 비효율적인 에너지 전달, 저하된 결정성 및 빠른 결정 성장으로 인한 구조적 결함으로 인해 비방사성 재결합이 증가하고 장치 성능이 크게 떨어집니다. 이 논문에서는 페로브스카이트의 결함을 최소화하기 위해 열 처리 공정을 통해 준 2차원 페로브스카이트의 결정 성장을 조정했습니다. 한편, 입자 크기는 열 처리 공정의 환경 조건을 조절하여 제어할 수 있으며, 이를 통해 방출 파장을 507-509nm 범위 내에서 조정할 수 있습니다. 열 처리 공정 조건을 최적화함으로써 준 2차원 페로브스카이트 발광 다이오드의 성능은 최대 휘도 4730 cd m^{-2} , 방출 파장이 513 nm에서 최대 외부 양자 효율 15.5%를 나타냈습니다. 준 2차원 페로브스카이트의 결정 성장 제어는 페로브스카이트 발광 다이오드의 차세대 디스플레이 소재로서 한단계 더 성장시킬 수 있습니다.

Acknowledgement

지금 이 문장을 작성하기 시작하며, 시간이 참 빠르다는 것을 느끼고 있습니다. 학부 3 학년 9 월부터 시작한 연구실 생활이 지금 학위 논문을 마무리하며 새 출발을 위해 정리가 되어갑니다. 연구실에서 지낸 지난 시간을 정리하며 연구에 대해 아무것도 모르던 때에 비해 스스로에게 많은 변화가 일어났음을 느낄 수 있었습니다. 지금에 이르기까지 많은 도움을 주신 분들께 감사의 인사를 전하고자 합니다.

우선, 현재 제가 소속 되어있는 ODPL에서 잘 적응할 수 있도록 좋은 환경을 제공해주시고, 연구에 있어 조언이 필요할 때면 아낌없는 조언을 해 주시며 많은 격려를 주셨던 지도교수님 박성흠 교수님께 또한 감사의 말씀을 전합니다. 저에게 항상 연구실 생활에 불편한 점은 없는지, 연구에 있어 도움이 필요한 지 물어봐 주시며, 이러한 아낌없는 관심과 배려에 정말 감사드립니다. 그리고 저에게 연구에 대해 하나부터 열까지 차근 차근 알려주시며 제가 스스로 연구의 즐거움을 느낄 수 있도록, 그리고 제가 원하는 연구를 할 수 있도록 아낌없는 지원과 연구에 대해 함께 고민을 해 주시며 많은 조언해 주신 이보람 교수님께 진심을 담아 감사의 말씀을 드리고 싶습니다. 부경대학교 물리학과에서 처음 수업을 들을 때부터 연구실 생활을 마무리하기 까지, 심지어 서울에서 바쁘신 와중에도 항상 챙겨주시고 배려해 주신 덕분에 여기까지 올 수 있었습니다. 학부 생활 동안 그저 성적만을 위한 공부밖에 할 줄 모르며, 스스로 무언가를 직접 이루고자 하는 목표가 없던 제가 석사를 마무리하는 이 순간까지 올 수 있도록 이끌어 주셨던 모든 순간들, 주셨던 두 분의 모든 가르침들은 앞으로의 제 인생에 있어 잊지 못할 가장 중요한 순간들과 가르침이 될 것입니다.

제 연구실 생활이 진행되는 동안 함께 실험을 진행하며 많은 조언과 관심을 주시고, 함께 고민을 해 주시며 많은 도움을 주신 HOME 연구실 모든 분들께 감사의 말씀을 드립니다. 또한 ODPL 연구실에 소속되며 잘 적응할 수 있도록, 그리고 연구를 잘 할 수 있도록 편안한 환경을 조성해 주신 ODPL 연구실 분들께 감사를 포함합니다. 함께 했던 모든 순간들이 저에게 있어 앞으로의 행보에 있어 소중한 추억들이 될 것 같습니다.

마지막으로, 석사 학위를 받을 때까지 저를 믿어주고 아낌없는 지원을 해 주신 저의 가족에게 깊은 감사의 마음을 포함합니다. 앞으로 더욱 열심히 노력하고 스스로를 성장시키며 좋은 모습을 보여드릴 수 있도록 노력하겠습니다. 항상 사랑하고, 감사의 마음을 전합니다.